

Fatigue Crack Paths in Notched Shells

Andrea Carpinteri, Roberto Brighenti, Andrea Spagnoli and Sabrina Vantadori

Department of Civil and Environmental Engineering & Architecture
University of Parma - Parco Area delle Scienze 181/A – 43100 Parma – Italy
E-mail: andrea.carpinteri@unipr.it

ABSTRACT. *An external surface flaw is assumed to be located at the root of a notch in a metallic double-curvature thin-walled shell subjected to an internal pressure. This defect presents an elliptical-arc shape with the ellipse aspect ratio changing during the whole crack propagation, as has experimentally been observed. An approximate expression of the stress-intensity factor along the crack front is deduced by applying the finite element method and the superposition principle. Then a numerical procedure is carried out to predict the crack growth for cylindrical and spherical shells under cyclic internal pressure. Some results are compared with those determined by other Authors for unnotched shells.*

INTRODUCTION

Structural safety of pressure vessels, such as pipes, elbows, closures, should be assessed also by taking into account the influence of flaws, inclusions, cracks and so on [1-10]. As a matter of fact, these defects can remarkably affect the reliability of such components, especially when they are subjected to time-varying loading and in presence of stress concentrators (holes, notches, etc.).

In the present paper, a part-through-cracked notched double-curvature thin-walled shell is represented as a part of a toroidal shell. The notch profile is assumed to belong to one of the two planes defined by the principal curvature radii of the shell. An external surface defect may initiate because of damage or stress concentration, and propagate under cyclic loading. Such a part-through flaw is assumed to be located at the notch root, to lie in one of the above two planes, and to present an elliptical-arc shape.

Firstly, seven elementary opening stress distributions (constant, linear, quadratic, cubic, quartic, fifth and sixth order) acting on the crack faces are considered. The finite element (FE) method is applied to determine the Stress-Intensity Factor (SIF) along the crack front for different values of the Stress Concentration Factor (SCF). Then, approximate SIFs in cracked cylindrical, toroidal and spherical shells under internal pressure are computed through the SIFs obtained for the seven elementary stresses above, by employing the superposition principle and the power series expansion of the stress fields determined in uncracked structural components analogous to the cracked ones being examined.

Finally, a numerical procedure is carried out to predict the crack path under cyclic internal pressure with the loading ratio equal to zero. Some results are compared with those available in the literature for unnotched shells.

NOTCHED SHELL WITH A SURFACE CRACK

A portion of a thin-walled shell is assumed to be a part of a shell of revolution, whose external surface presents two principal curvature radii equal to R_1 and R_2 (Figs 1 and 2). The parameters t , c and ρ represent the wall thickness of the shell, the notch depth, and the notch radius, respectively, whereas $t' = t - c$ is the reduced wall thickness in the notched zone. The circular-arc notch is located in one of the two planes defined by the principal curvature radii of the shell being examined. The dimensionless wall thickness, $R^* = (R_1 - t)/t$, of the shell is assumed to be equal to 10.

An external surface flaw is assumed to belong to one of the two planes defined in the previous paragraph. Note that the principal curvature radius of the shell in the crack plane is called R_1 , whereas the other principal curvature radius at the same point F is called R_2 (Fig. 1). The dimensionless relative curvature radius $r = R_1/R_2$ is herein used to indicate different configurations: in particular, the defect can be considered as a transversal surface flaw for $R_1 < R_2$ ($r < 1$), and as a longitudinal one for $R_1 > R_2$ ($r > 1$).

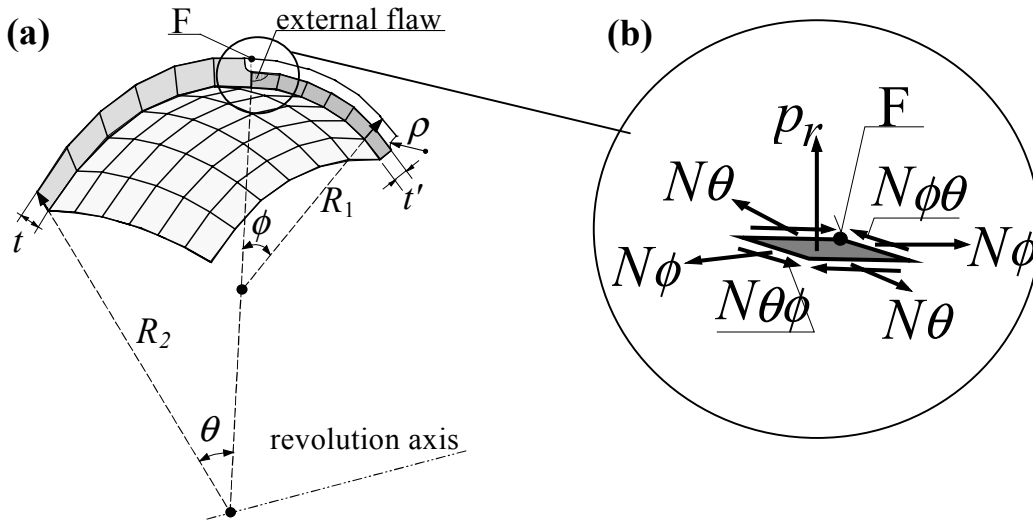


Figure 1. Geometrical parameters (a); forces acting on an infinitesimal shell portion (b).

The equilibrium of an unnotched thin-walled portion of a shell (Fig. 1b) can be described by the classical shell theory. The equilibrium equations along the meridional, parallel and radial directions, respectively, for the infinitesimal shell portion are given by:

$$\begin{aligned} (R_2 N_\phi)_{,\phi} + R_1 (N_{\theta\phi})_{,\theta} - R_1 N_\theta \cos\phi + p_\phi R_2 R_1 &= 0 \\ (R_2 N_{\phi\theta})_{,\phi} + R_1 (N_\theta)_{,\theta} + R_1 N_{\theta\phi} \cos\phi + p_\theta R_2 R_1 &= 0 \\ N_\phi / R_1 + N_\theta / R_2 - p_r &= 0 \end{aligned} \quad (1)$$

where the notations $(\bullet)_{,\phi}$ and $(\bullet)_{,\theta}$ denote the partial derivatives with respect to the angles ϕ and θ , respectively.

For notched shells, the stress field cannot be determined in a closed form, and a numerical evaluation is required. In the following, the cases of notched spherical and cylindrical shells under an internal pressure are examined. Once the stresses are known (analytically or numerically), they can be used to calculate approximate values of K_I along the crack front for cracked shells.

STRESS-INTENSITY FACTOR (SIF) DETERMINATION

The external surface flaw being considered is assumed to present an elliptical-arc shape ($\alpha = a/b =$ flaw aspect ratio, $\xi = a/t_h =$ relative crack depth, where t_h is equal to t for an unnotched shell and to t' for a notched one, respectively, Fig. 2), to be located at the notch root, and to belong to one of the two planes defined by the principal curvature radii of the shell being examined. The generic point P on the crack front is identified by the dimensionless coordinate $\zeta^* = \zeta/h$.

Various situations can occur (Fig. 3) : the defect is longitudinal-like for $R_1 > R_2$ (cases (b) and (c)) and transversal-like for $R_1 < R_2$ (cases (e) and (f)), while the particular case of $R_1 = R_2$ ((a) and (d)) refers to a portion of a spherical shell for which it is meaningless to distinguish between a transversal flaw and a longitudinal flaw.

By employing the power series expansion of the actual stresses in a given body and the superposition principle, an approximate SIF can be computed for any actual loading. In order to obtain a wide range of useful stress-intensity factors, seven elementary stress distributions perpendicular to the crack faces are considered :

$$\sigma_{I(n)} = (w/a)^n = \eta^n \quad n = 0, \dots, 6 \quad (2)$$

where w is the radial coordinate, with its origin on the circular arc (having radius u) belonging to the crack plane and passing through the deepest point A of the crack front (Fig. 2), whereas $\eta = w/a$ is the dimensionless radial coordinate.

The dimensionless Mode I stress-intensity factor for the n-th elementary stress distribution is computed as follows :

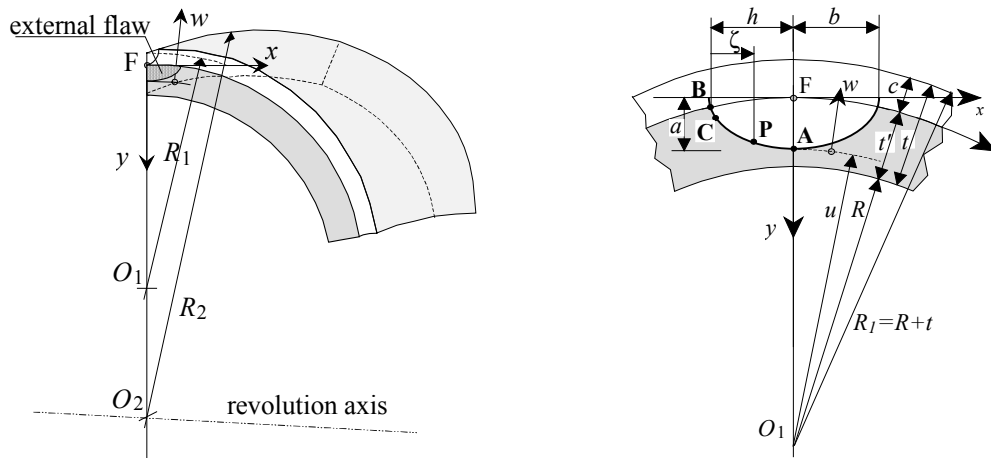


Figure 2. External surface flaw in a portion of a double-curvature notched shell.

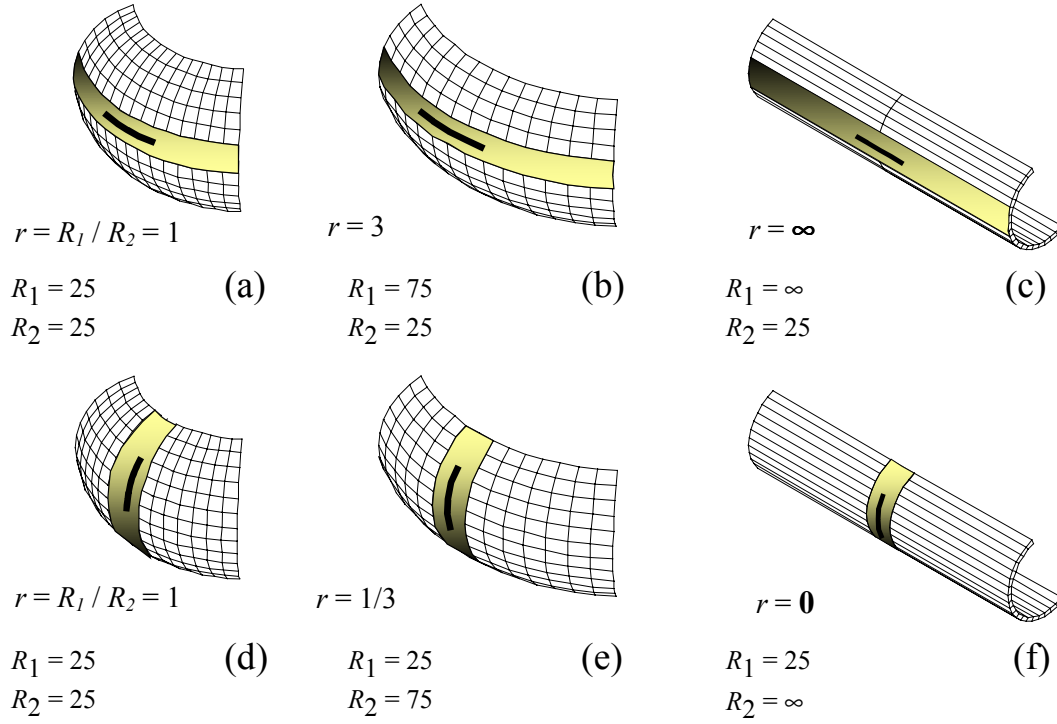


Figure 3. External longitudinal-like (a)-(c) and transversal-like (d)-(f) surface flaw in a notched shell (sizes in mm). The coloured area indicates the notch location.

$$K^*_{I(n)} = K_{I(n)} / (\sigma_{ref(n)} \sqrt{\pi a}) \quad (3)$$

where $\sigma_{ref(n)} = 1$ and $K_{I(n)}$, related to the n -th load case, is obtained from a FE analysis.

An approximate expression of the dimensionless SIF for a complex stress distribution, $\sigma_{I(L)}(w)$, where the subscript (L) indicates the generic load case, is given by [8]:

$$K^*_{I(L)} = \frac{1}{\sigma_{ref(L)}} \cdot \sum_{n=0}^6 B_{n(L)} \cdot K^*_{I(n)} \quad (4)$$

with the coefficients $B_{n(L)}$ expressed by :

$$B_{n(L)} = a^n \cdot \left[\frac{1}{n!} \cdot \frac{d^{(n)} \sigma_{I(L)}(w)}{d(w)^{(n)}} \right] \quad (5)$$

whereas $\sigma_{ref(L)}$ is the reference stress for the the generic load case (L) considered.

In the following, two particular shells (cylindrical and spherical) subjected to an internal pressure are examined.

SIFs FOR CYLINDRICAL AND SPHERICAL SHELLS

Cylindrical Shell under Internal Pressure

The actual hoop stress distribution, $\sigma_{I(p,cu)}$, in an *unnotched* cylinder ($R_1 = \infty, R_2 = 25$ mm, $r = \infty$) under an internal pressure p can be written as follows [11]:

$$\sigma_{I(p,cu)}(w) = \frac{p (R_2 - t)^2}{R_2^2 - (R_2 - t)^2} \left(\frac{R_2^2}{(R_2 + w - a)^2} + 1 \right) \quad (6)$$

For a longitudinal surface flaw, an approximate expression of the dimensionless SIF, $K^*_{I(p,cu)}$, along the crack front can be determined through the superposition principle (see Eq.4, [8]) :

$$K^*_{I(p,cu)} = \frac{1}{\sigma_{ref(p,cu)}} \sum_{n=0}^5 B_{n(p,cu)} K^*_{I(n)} \quad (7)$$

where $\sigma_{ref(p,cu)} = p \bar{R} / t$ is the well-known uniform hoop stress in a thin-walled pipe under internal pressure (\bar{R} = mean radius of the cylinder), and the coefficients $B_{n(p,cu)}$ (see Eq. 5) are listed in Table 1.

Table 1. Coefficients of series expansion for a cylindrical shell under an internal pressure.

$\sigma_{I(p,cu)}(w) = \frac{p (R_2 - t)^2}{R_2^2 - (R_2 - t)^2} \cdot \left[\frac{R_2^2}{(R_2 + w - a)^2} + 1 \right]$	$B_0(p,cu) = \frac{p (R_2 - t)^2}{R_2^2 - (R_2 - t)^2} \cdot \left[\frac{R_2^2}{(R_2 - a)^2} + 1 \right]$
$B_1(p,cu) = \frac{-2p (R_2 - t)^2}{R_2^2 - (R_2 - t)^2} \cdot \frac{R_2^2}{(R_2 - a)^3} \cdot a$	$B_2(p,cu) = \frac{3p (R_2 - t)^2}{R_2^2 - (R_2 - t)^2} \cdot \frac{R_2^2}{(R_2 - a)^4} \cdot a^2$
$B_3(p,cu) = \frac{-4p (R_2 - t)^2}{R_2^2 - (R_2 - t)^2} \cdot \frac{R_2^2}{(R_2 - a)^5} \cdot a^3$	$B_4(p,cu) = \frac{5p (R_2 - t)^2}{R_2^2 - (R_2 - t)^2} \cdot \frac{R_2^2}{(R_2 - a)^6} \cdot a^4$
$B_5(p,cu) = \frac{-6p (R_2 - t)^2}{R_2^2 - (R_2 - t)^2} \cdot \frac{R_2^2}{(R_2 - a)^7} \cdot a^5$	

In the case of a *notched* cylindrical shell, the analytical solution for the hoop stress distribution $\sigma_{I(p,c)}(w)$ is not available. Therefore, $\sigma_{I(p,c)}(w)$ must numerically be computed in order to obtain the coefficients $B_{n(p,c)}$. The reference stress can conveniently be defined as $\sigma_{ref(p,c)} = p \bar{R} / t'$, and the dimensionless SIF, $K^*_{I(p,c)}$, can be obtained from an expression similar to Eq. 7, where the subscript *cu* is replaced by *c*.

Spherical Shell under Internal Pressure

In the case of an *unnotched* spherical shell ($R_1 = R_2 = R_s$, $r = 1$) under an internal pressure p , the actual hoop stress distribution $\sigma_{I(p,su)}$ along the wall thickness is given by [11] :

$$\sigma_{I(p,su)}(w) = \frac{p \cdot (R_s - t)^3}{2(R_s + w - a)^3} \cdot \frac{R_s^3 + 2(R_s + w - a)^3}{R_s^3 - (R_s - t)^3} \quad (8)$$

An approximate dimensionless SIF, $K^*_{I(p,su)}$, is deduced by using the superposition principle (see Eq.4, [8]):

$$K^*_{I(p,su)} = \frac{1}{\sigma_{ref}(p,su)} \sum_{n=0}^6 B_n(p,su) K^*_{I(n)} \quad (9)$$

where $\sigma_{ref}(p,su) = p\bar{R} / (2t)$ is the well-known hoop stress in a pressurised thin-walled sphere (\bar{R} = mean radius of the sphere), and the coefficients $B_n(p,su)$ (see Eq. 5) are listed in Table 2.

Table 2. Coefficients of series expansion for a spherical shell under an internal pressure.

$\sigma_{I(p,su)}(w) = \frac{p \cdot (R_s - t)^3}{2(R_s + w - a)^3} \cdot \frac{R_s^3 + 2(R_s + w - a)^3}{R_s^3 - (R_s - t)^3}$	$B_0(p,su) = \frac{p(R_s - t)^3(R_s^3 + 2(R_s - a)^3)}{2(R_s - a)^3(R_s^3 - (R_s - t)^3)}$
$B_1(p,su) = \frac{3pa(R_s - t)^3}{(R_s - a)(R_s^3 - (R_s - t)^3)} \left[1 + \frac{R_s^3 + 2(R_s - a)^3}{2(R_s - a)^3} \right]$	$B_2(p,su) = \frac{3pa^2(R_s - t)^3}{(R_s - a)^2(R_s^3 - (R_s - t)^3)} \left[-2 + \frac{R_s^3 + 2(R_s - a)^3}{(R_s - a)^3} \right]$
$B_3(p,su) = \frac{5pa^3(R_s - t)^3}{(R_s - a)^3(R_s^3 - (R_s - t)^3)} \left[2 + \frac{R_s^3 + 2(R_s - a)^3}{(R_s - a)^3} \right]$	$B_4(p,su) = \frac{15pa^4(R_s - t)^3}{(R_s - a)^4(R_s^3 - (R_s - t)^3)} \left[1 + \frac{R_s^3 + 2(R_s - a)^3}{2(R_s - a)^3} \right]$
$B_5(p,su) = \frac{21pa^5(R_s - t)^3}{(R_s - a)^5(R_s^3 - (R_s - t)^3)} \left[1 + \frac{R_s^3 + 2(R_s - a)^3}{2(R_s - a)^3} \right]$	$B_6(p,su) = \frac{14pa^6(R_s - t)^3}{(R_s - a)^6(R_s^3 - (R_s - t)^3)} \left[2 + \frac{R_s^3 + 2(R_s - a)^3}{(R_s - a)^3} \right]$

In the case of a *notched* spherical shell, the analytical solution for the hoop stress distribution $\sigma_{I(p,s)}(w)$ is not available. Therefore, $\sigma_{I(p,s)}(w)$ must numerically be computed in order to obtain the coefficients $B_n(p,s)$. The reference stress can conveniently be defined as $\sigma_{ref}(p,s) = p\bar{R} / (2t')$, and the dimensionless SIF, $K^*_{I(p,s)}$, can be obtained from an expression similar to Eq. 9, where the subscript *su* is replaced by *s*.

CRACK PROPAGATION IN CYLINDRICAL AND SPHERICAL SHELLS

The above approximate SIFs are displayed in Figs 4a and 4b for unnotched and notched cylindrical shells, respectively, whereas results for unnotched and notched spherical shells are plotted in Figs 4c and 4d, respectively. Note that in the *unnotched* case the SIF increases with ξ for both point A and point C, while in the *notched* case the SIF may either increase, or decrease or have a non-monotonic trend with increasing ξ . The curves shown in Fig. 4d are truncated at $\xi \cong 0.44$, since the polynomial fitting (using seven terms, i.e. $n=0, \dots, 6$) of the real stress distribution in the notched cross-section of the spherical shell gives us a good approximation of the actual stress field for ξ ranging from 0.0 to about 0.44.

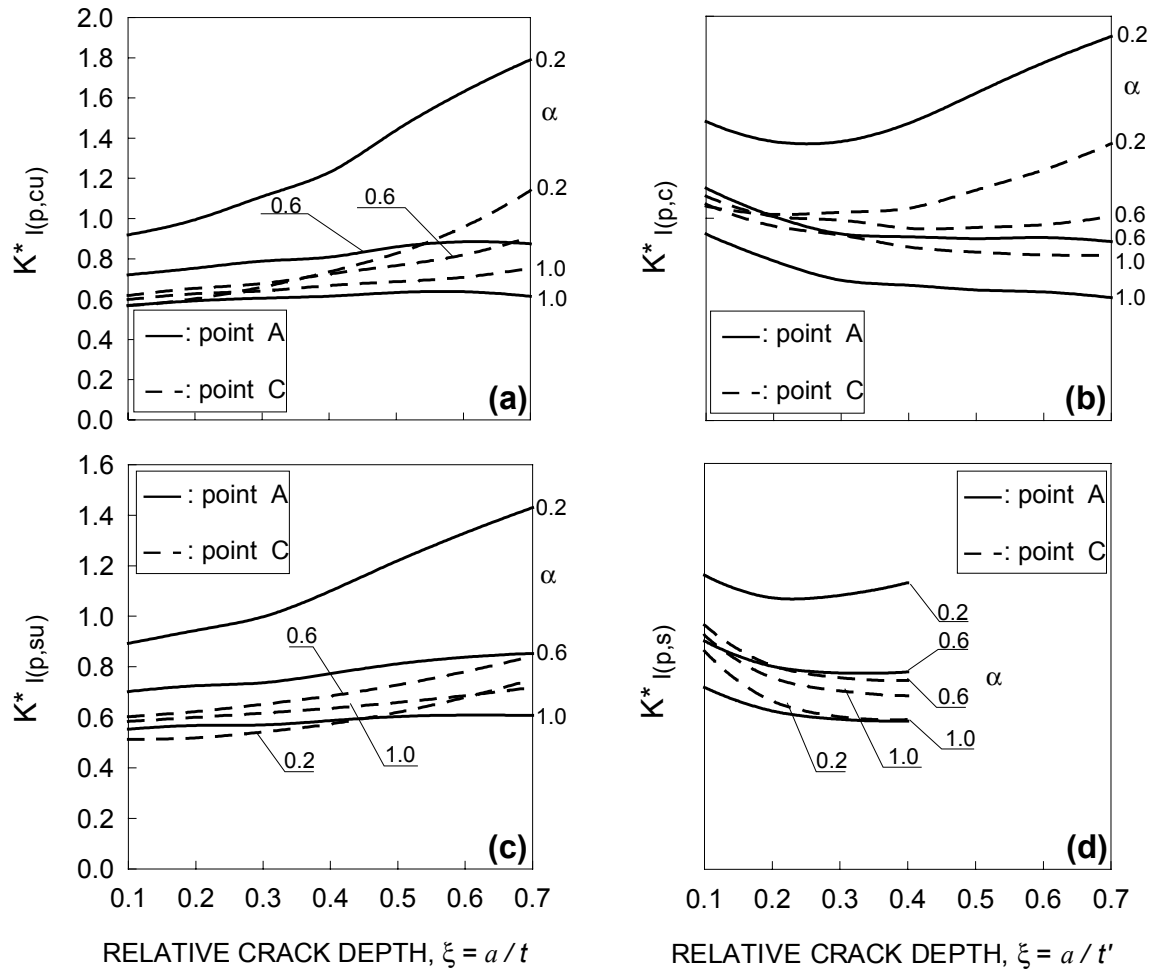


Figure 4. SIFs under internal pressure, at the deepest A and the surface point C in: (a) an unnotched ($r = \infty, \rho_d = \infty$) and (b) a notched ($r = \infty, \rho_d = 0.1$) cylindrical shell; (c) an unnotched ($r=1, \rho_d = \infty$) and (d) a notched ($r=1, \rho_d = 0.1$) spherical shell.

Now the SIF results are used for fatigue crack growth predictions. A cylindrical shell ($r = \infty$) and a spherical shell ($r = 1$) under cyclic internal pressure with constant amplitude are examined by employing a two-parameter theoretical model [4]. Diagrams of α against ξ are shown in Fig. 5, for six initial crack configurations. Results by Lin et al. [7] are also reported for a cylindrical unnotched shell (Fig. 5a).

It can be observed that the flaws considered tend to follow preferred fatigue propagation paths for both cylindrical and spherical shells. Note that, for a given value of ξ in Figs 5a and 5c, the values of α for notched shells (dashed line) are considerably lower than those for unnotched shells (continuous line).

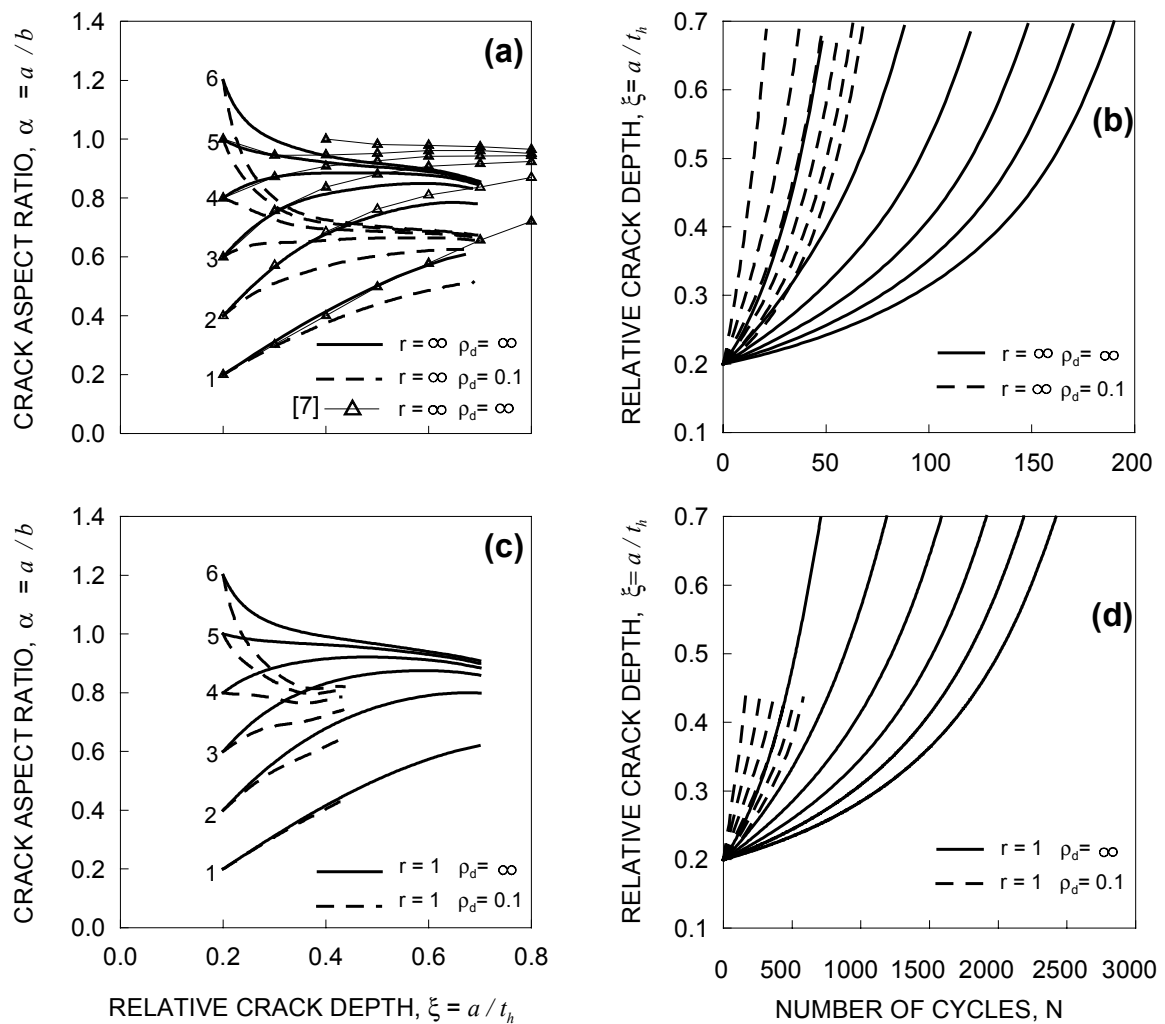


Figure 5. Unnotched and notched cylindrical ($r = \infty$) and spherical ($r = 1$) shells under cyclic internal pressure: crack propagation paths (a and c) and life estimation (b and d; the loading cycles, N , have been divided by 10^3).

CONCLUSIONS

The behaviour of a part-through-cracked notched shell under an internal pressure has been examined. The damaged zone can conveniently be represented by a portion of a shell of revolution with principal curvature radii equal to R_1 and R_2 , whereas the defect is assumed to present an elliptical-arc shape with flaw aspect ratio $\alpha = a/b$ and relative crack depth $\xi = a/t_h$. The stress-intensity factor (SIF) distribution has numerically been determined for different values of the relative curvature radius $r = R_1/R_2$. As an example, the SIFs for cylindrical ($r = \infty$) and spherical ($r = 1$) shells under internal pressure have been plotted. Note that the SIF for an unnotched shell increases with ξ , while the SIF for a notched shell may either increase, or decrease or have a non-monotonic trend with increasing ξ .

Finally, for cylindrical and spherical shells under cyclical internal pressure, fatigue crack paths have been deduced by employing a two-parameter theoretical model [4]. The surface flaws considered follow preferred propagation paths in the diagram of α against ξ . The notch effect consists in a reduction of the fatigue life and the flaw aspect ratio (i.e. the crack front tends to flatten with respect to that for an unnotched shell).

ACKNOWLEDGEMENTS

The authors gratefully acknowledge the research support for this work provided by the Italian Ministry for University and Technological and Scientific Research (MIUR).

REFERENCES

1. Raju, I.S. and Newman, J.C., Jr. (1982) *J. Pressure Vessel Tech.* **104**, 293-298.
2. Pook, L.P. (1983) *The Role of Crack Growth in Metal Fatigue*. Metals Society, London.
3. Joseph, P.F. and Erdogan, F. (1988) *J. Applied Mech.* **55**, 795-804.
4. Carpinteri, A. (1993) *Int. J. Fatigue* **15**, 21-26.
5. Carpinteri, A. (Editor) (1994) *Handbook of Fatigue Crack Propagation in Metallic Structures*. Elsevier Science Publishers B.V., Amsterdam, The Netherlands.
6. Joseph, P.F., Cordes, R. D. and Erdogan, F. (1995) *Nuclear Engng Design* **158**, 263-276.
7. Lin, X.B. and Smith, R.A. (1997) *Int. J. Pressure Vessels Piping* **71**, 293-300.
8. Carpinteri, A., Brighenti, R. and Spagnoli, A. (2000) *Fatigue Fract. Engng Mater. Struct.* **23**, 467-476.
9. Brighenti, R. (2000) *Int. J. Fatigue* **22**, 559-567.
10. Pook, L.P. (2002) *Crack Paths*. WIT Press, Southampton.
11. Timoshenko, S.P. and Goodier, J.N. (1970) *Theory of elasticity*. McGraw-Hill Book Company.